Thermodynamic Analysis of AlSi10Mg Alloy

Termodinamična analiza zlitine AlSi10Mg

Maja Vončina, Primož Mrvar, Jožef Medved

Faculty of material science and engineering, Department of materials and metallurgy,
University of Ljubljana, Aškerčeva 12, 1000 Ljubljana, Slovenija;
E-mail: jozef.medved@ntf.uni-lj.si

Received: July 25, 2005 **Accepted:** October 28, 2005

Abstract: The AlSi10Mg alloy is one of the most frequently used alloys for different purposes because of its suitable mechanical properties. The alloy was examined with chemical analyses, with the triple simple thermal analysis (TSTA), the simultaneous thermal analysis (STA), the computer simulation using Thermo-Calc program and with the metallographic analyses.

The triple simple thermal analysis has been performed in three measuring cells simultaneously, with different cooling rates. High cooling rates simulated the actual cooling rate in the die casting process. Chemical analyses were used to verify whether the concentration of alloying elements is in suitable limits. Metallographic analyses enabled us to define phases in the microstructure at different cooling rates and they were verified with the Thermo-Calc computer simulation method. Research showed that the alloy should contain the amount of silicon near to the highest limit and a suitable concentration of manganese, which prevents the formation of needle β-Al_5FeSi phase and enables formation less harmful α-$Al_{15}(MnFe)_3Si_2$ phase. The triple simple thermal analysis showed that higher cooling rate has beneficial influence on the development of microstructure.

Key words: Al-alloy, thermodynamics, solidification, triple simple thermal analysis.

Introduction

The AlSi10Mg alloy is used for making complicated, heavy-duty castings with thick walls for aircraft, vehicle, chemical and food industry. It is suitable for sand casting, mould casting, and die casting. At casting of Al alloys often defects appear which cause that the casting is unsuitable. Reasons for casting defects and defects in the structure of the material can be found in the melt preparation technology and in the casting procedure itself.

Technically significant aluminium casting alloys are developed from the Al-Si binary system being extended with some other alloying elements to improve mechanical and other properties where it becomes important the process of precipitation. Excellent castability of aluminium casting alloys enables to produce castings of complicated shapes. Alloying the magnesium to the binary Al-Si alloys enables precipitation of alloy and attainment of prescribed mechanical properties.

Scientific paper

For a reliable production of castings with prescribed properties we have to get insight into the course of solidification, development of microstructure and the structure of the alloy, which in practice represents bigger or smaller difficulties. To accomplish this purpose we have laboratorically examined AlSi10Mg alloys of three different manufacturers (Z1, Z2 and Z3). Foundries usually use chemical analyses for control of the melt, and optical and electron microscopy for control of the final castings. We have examined our alloys with chemical analyses, with the TSTA, the STA, with the computer simulation using the Thermo-Calc program, and with the metallographic analyses. The minimum and maximum liquidus temperatures - $T_{L/min}$ and $T_{L/max}$, minimum and maximum eutectic temperatures – $T_{E/min}$ and $T_{E/max}$, temperatures of completed solidification – T_K, and the temperatures of precipitation of the Mg_2Si phase were determined.

Crystallography of AlSi10Mg alloy

Aluminium and silicon are showing limited mutual melting and they form a eutectic system with the eutectic point at 12.6 mass % Si and at temperature 577 °C.

Silicon as an alloying element causes small contractions during the cooling and solidification[1]. Concentration of silicon in aluminium alloys is 5 to 25 %[1]. With alloying magnesium to the binary alloys Al-Si the heat precipitation of the alloy is enabled.

It is necessary to prepare the melt before the casting process, because of its influence on the quality of final castings. Preparation of the melt before the alloying mainly consists of cleaning the melt to remove impurities, to degas and modify the melt in order to obtain the required shape, size and distribution of microstructure components and phases[1,2].

The chemical composition of the casting alloy is presented in Table 1[1]. The alloy

Table 1. Chemical composition of alloy AlSi10Mg ISO (3522 AlSi10Mg (R164)) [1].
Tabela 1. Kemijska sestava zlitine AlSi10Mg po ISO 3522 AlSi10Mg (R164).

Si	Fe	Cu	Mn	Mg	Zn	Other elements	Difference
9.0-10.0	0.6	0.1	0.05	0.45-0.6	0.05	0.15	Al

Table 2. Possible reactions during solidification of Al-Si-Mg alloy[1].
Tabela 2. Reakcije, ki lahko potekajo med strjevanjem zlitine Al-Si-Mg.

Reaction		Temp. [°C]
e_1	$l \Leftrightarrow (Al) + Mg_2Si$	593
e_2	$l \Leftrightarrow Al_3Mg_2 + Mg_2Si$	
e_3	$l \Leftrightarrow Al_{12}Mg_{17} + Mg_2Si$	
E_1	$L \Leftrightarrow (Al) + Mg_2Si + (Si)$	550
E_2	$L \Leftrightarrow (Al) + Al_3Mg_2 + Mg_2Si$	444
E_3	$L \Leftrightarrow Al_3Mg_2 + Al_{30}Mg_{23}(HT) + Mg_2Si$	445
E_4	$L \Leftrightarrow Al_{12}Mg_{17} + (Mg) + Mg_2Si$	434
U_1	$L + Al_{12}Mg_{17} \Leftrightarrow Al_5Mg_4 + Mg_2Si$	452
U_2	$L + Al_5Mg_4 \Leftrightarrow Al_{30}Mg_{23}(HT) + Mg_2Si$	448

belongs to the Al corner of the ternary system Al-Si-Mg, where the following equilibria occur: L> α_{Al}, L > α_{Al} + $\beta_{Si,}$ and ternary eutectic L > α_{Al} + Mg_2Si + β_{Si} (Figure 1) [2]. In alloys of Al-Si-Mg system the process of solidification can be performed over the reactions that are shown in Table 2.

Depending on the cooling rate, especially for in practice typical larger cooling rates, dendritic shape primary crystals multi-component solid solution α_{Al} can be obtained in the microstructure in the first stage of solidification (Figure 2a) [1], because of alloying elements like iron and manganese, we can trace in the microstructure labyrinthine phase α_{Al}-$Al_{15}(MnFe)_3Si_2$ (Figure 2b)[1,2].

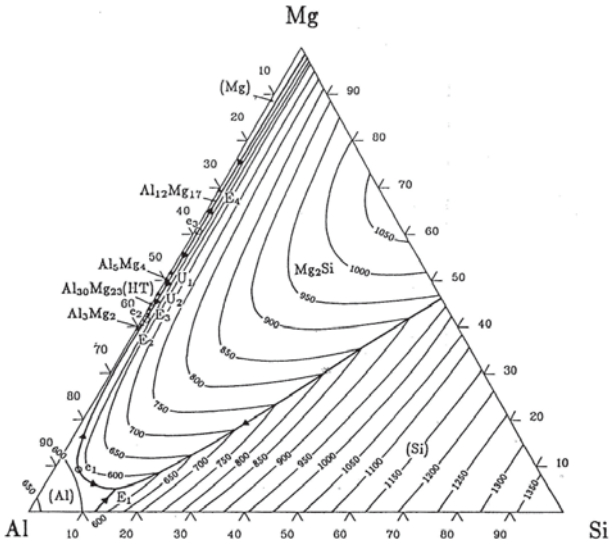

Figure 1. Liquid surface of the ternary system Al-Si-Mg[7].
Slika 1. Likvidus ploskev ternarnega sistema Al-Si-Mg.

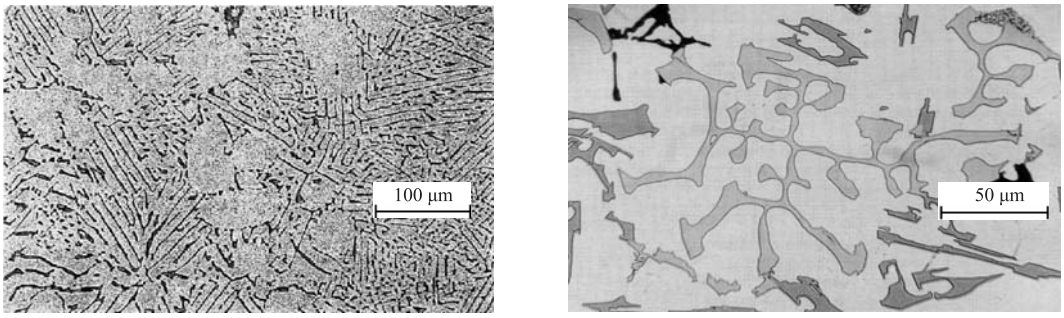

a) b)

Figure 2. Microstructure of AlSi10Mg alloy: a) Primary crystal of solid solution a_{Al} dendritic shape and eutectic (a_{Al} + b_{Si}), b) Dendritic phase of a_{Al} and a-$Al_{15}(MnFe)_3Si_2$ phase (labyrinthine) and Mg_2Si (black) [7].
Slika 2. Mikrostruktura zlitine AlSi10Mg: a) Primarni kristali trdne raztopine a_{Al} v obliki dendritov ter evtektik (a_{Al} + b_{Si}), b) Dendriti faze a_{Al} ter faza a-$Al_{15}(MnFe)_3Si_2$ (labirintasto) in Mg_2Si (črno).

EXPERIMENTAL

In the present research we used standard blocks of AlSi10Mg alloy of three different manufacturers with composition, shown in Table 3.

TSTA measurements were carried out in three different cells simultaneously. Each measurement was performed three times. Figure 3 shows the measuring cells used in TSTA. We used two measuring cells made of gray cast iron with lamellar graphite, while the third cell was made by the Croning process. The first measuring cell, made of gray cast iron with lamellar graphite**,** had a diameter of 30 mm and volume of 33.807 mm^3, the second one, made of the same materials, had a diameter of 15 mm and volume of 8.062 mm^3, while the third cell, made of sand, had the same dimensions as the first one. We have put the K-type thermocouples in the center and at the same height of each measuring cell, as shown in Figure 3. The prepared alloys were melted in graphite crucibles in an induction furnace. As the temperature 750 °C was reached, the melt was poured from the graphite crucible into the three measuring cells. The thermocouples were connected to the National Instruments DAQPad-MI0-16XE–50 measuring card, and this to the personal computer, where the measured values were collected with the LabVIEW 5.0 program. Cooling curves were plotted using the Origin 6.0 program. Different geometries and materials of the measuring cells caused various heat transfers, and, consequentially, different cooling rates.

Simultaneous thermal analysis of specimens of starting materials was performed on the STA 449 NETZSCH machine. We put together two equal cups made of corundum to the platinum sensor. In one cup there was the examined material, in the other one the reference material. The measurements were carried out in a protective atmosphere of inert gas 99.999 % pure nitrogen. The specimens were heated up to 720 °C with heating rate of 10 K/min and cooled with the same cooling rate to the room temperature.

Thermodynamic equilibrium of the alloys Z1, Z2 and Z3 of three different manufacturers were simulated with the computer Thermo-Calc application. A suitable database in the program and the elements that composed our alloy were chosen. Our next step was to determine the amount of elements and to define the temperatures and pressures of the simulated equilibrium. The program has recorded all the thermodynamically possible phases that were present at defined conditions, and it constructed the equilibrium binary phase diagram. For all the alloys, the phases of completed solidification were simulated.
The chemical analyses of starting materials made by the Z1, Z2 and Z3 manufacturers and of the specimens after the TSTA were made. The specimens for the metallographic

Table 3. Chemical composition of alloy from three different manufacturers; mass %.
Tabela 3. Kemijska sestava zlitin treh različnih proizvajalcev; mas. %.

	Al	Cr1	Mg	Mn1	Cu	Zn	Ti	Ni3	Fe2	Si2	Pb
Z1	88.4888	0.0484	0.2999	0.1198	0.0815	0.0415	0.0092	0.0249	0.6504	10.2216	0.0067
Z2	87.5246	0.0018	0.3458	0.0209	0.0239	0.0175	0.0137	0.0035	0.4593	9.9959	0.0086
Z3	88.0195	0.0034	0.3631	0.0176	0.0728	0.0626	0.0065	0.0221	0.4556	10.9168	0.0503

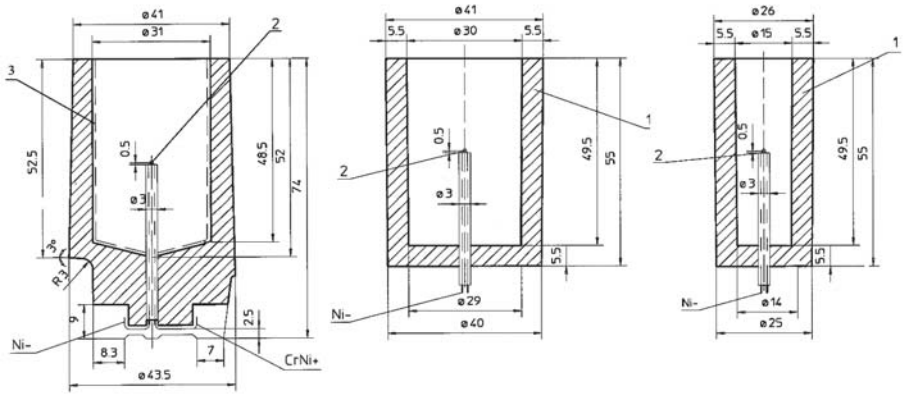

a) b) c)

Figure 3. Measuring cells: a) made by Croning sand, b) made by cast iron 30 mm diameter and c) made by cast iron 15 mm diameter; 1 - cast iron, 2 - thermocouples and 3 - coated.
Slika 3. Merilni lončki: a) iz Croning peska, b) iz sive litine premera 30 mm ter c) iz sive litine premera 15 mm; 1 - siva litina, 2 - termoelementi in 3 - s premazom.

analyses were cut from the specimens after the completed TSTA. The samples for the optical microscopy were prepared by the standard metallographic procedure. Prepared samples were observed and photographed in the Nikon Microphot FXA optical microscope that was equipped with the 3CCD-videocamera Hitachi HV-C20A and the analySIS computer program to analyze metallographic pictures.

Results And Discussion

Cooling curves and suitable microstructures of alloys from three different manufacturers are shown in Figures 4 - 6. Table 4 presents average temperatures of the TSTA. Table 4 reveals that the temperatures of the starting solidification, the minimum and maximum liquidus temperatures, and the minimum and maximum eutectic temperatures are

Table 4. Characteristic temperatures from triple simple thermal analyses; °C.
Tabela 4. Značilne temperature trojne enostavne termične analize; °C.

Alloy	Z1			Z2			Z3		
	a	**b**	**c**	**a**	**b**	**c**	**a**	**B**	**C**
T_N	640.5	633.0		647.5	639.3	631.0	629.8	626.3	633.5
T_L			588.0			578.5			575.5
$T_{L/min}$	582.3	581.8	576.5	584.5	582.3	577.3	575.3	575.2	571.5
$T_{L/max}$	586.5	584.0	579.8	589.0	584.5	579.5	579.8	581.7	575.8
dT_L	4.2	2.2	2.2	4.5	2.2	1.5	4.5	6.5	2.8
T_E			556.0				567.0	567.0	566.5
$T_{E/min}$	563.5	556.8	553.3	558.8	554.0	551.3	566.8	567.3	565.8
$T_{E/max}$	566.3	559.4	557.0	562.3	556.2	552.5	569.0	569.0	567.0
dT_E	2.8	2.6	2.5	3.5	2.2	1.2	1.5	1.2	0.8
T_K	542.8	550.2	531.0	548.8	545.0	531.0	542.8	550.8	533.0

decreasing with the increasing cooling rate. The highest liquidus undercooling was observed at the alloy Z3, the highest eutectic crystallizations undercooling at the alloy Z2.

With the STA, where the cooling rate was 10 K/min, temperatures of the starting solidification or liquidus temperature at cooling, and the temperatures of the initial melting or solidus temperature, at heating were determined. During cooling, the first to begin to solidify was the alloy Z1 (585.3 °C), then the alloy Z2 (585 °C), and the lowest liquidus temperature corresponded to the alloy Z3 (581.3 °C) (Figure 7a). Heating curves showed that the alloy Z3 had the lowest solidus temperature (543 °C), the alloy Z2 had a little higher solidus temperature (550 °C), and the highest solidus temperature belonged to the alloy Z1 (557 °C) (Figure 7b).

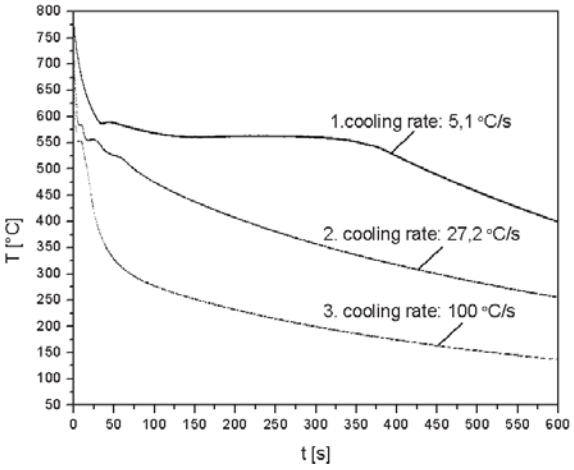

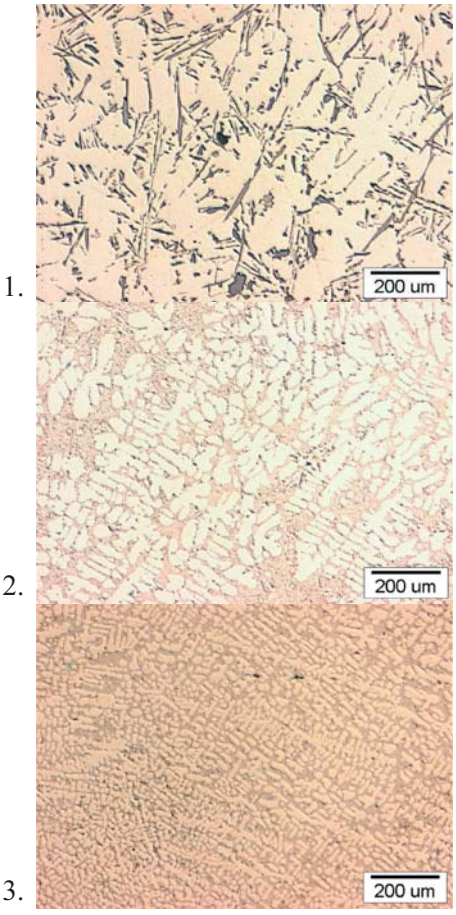

Figure 4. Cooling curves of AlSi10Mg alloy Z1 at three different cooling rates and their corresponding microstructure; 1. sand mould, Φ 30 mm; 2. cast iron mould, Φ 30 mm; 3. cast iron mould, Φ 15 mm.
Slika 4. Ohlajevalne krivulje zlitin AlSi10Mg Z1 pri treh ohlajevalnih hitrostih ter njihove ustrezne mikrostrukture; 1. peščena kokila, Φ 30 mm; 2. jeklena kokila, Φ 30 mm; 3. jeklena kokila, Φ 15 mm.

Using the Thermo-Calc program, the course of equilibrium solidification of the AlSi10Mg alloy was determined. The Si_2Ti phase started to solidify the first, followed by the α_{Al} phase (primary mixture crystals of solid solution based on aluminium). We can define the temperature of solidification of α_{Al} crystals as liquidus temperature of the alloy. From the melt, the Si and $Al_{13}Fe_4$ phases began to precipitate. When the eutectic temperature was reached, the remaining melt solidified as eutectic (α_{Al}+ β_{Si}). At the end, the Mg_2Si phase and $Al_{12}Mn$ and Al_2Cu phases precipitated from the solid solution.

Figure 8 shows characteristic temperatures at different cooling rates. Cooling rate of 0.01°C/s represented the equilibrium solidification that was achieved with the Thermo-Calc program. With STA the cooling

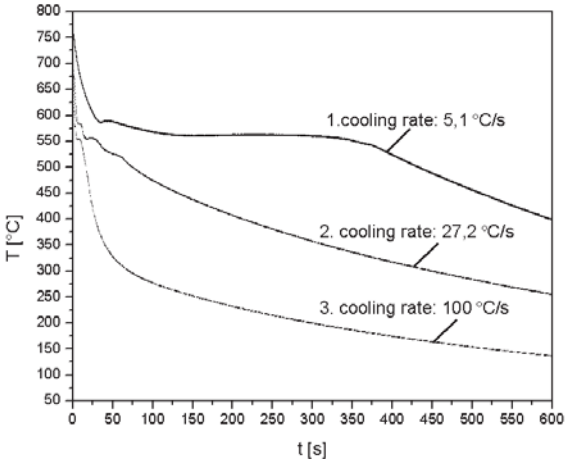

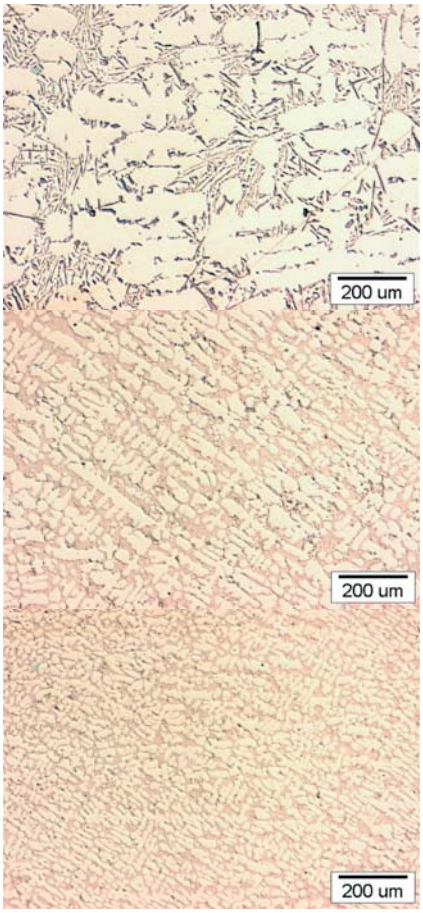

Figure 5. Cooling curves of AlSi10Mg alloy Z2 at three different cooling rates and their corresponding microstructure; 1. sand mould, Φ 30 mm; 2. cast iron mould, Φ 30 mm; 3. cast iron mould, Φ 15 mm.
Slika 5. Ohlajevalne krivulje zlitine AlSi10Mg Z2 pri treh ohlajevalnih hitrostih ter njihove ustrezne mikrostrukture; 1. peščena kokila, Φ 30 mm; 2. jeklena kokila, Φ 30 mm; 3. jeklena kokila, Φ 15 mm.

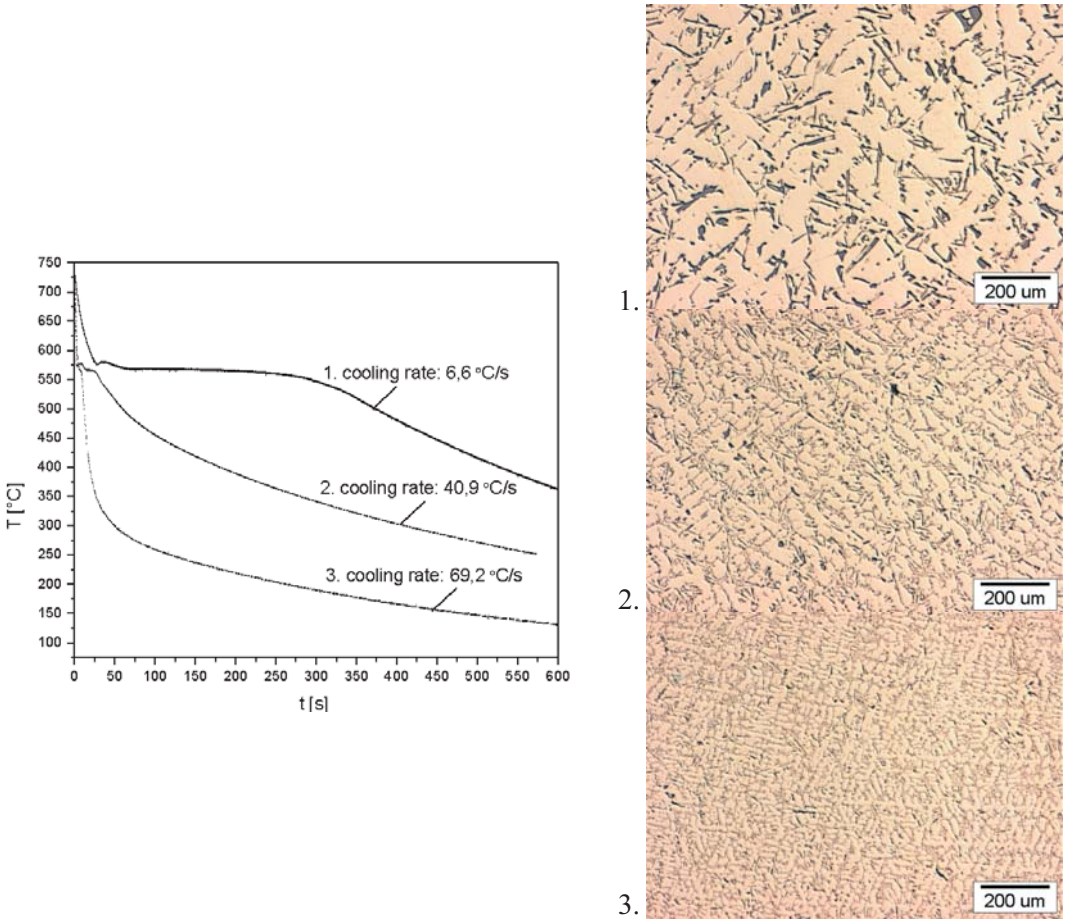

Figure 6. Cooling curves of AlSi10Mg alloy Z3 at three different cooling rates and their corresponding microstructure; 1. sand mould, Φ 30 mm; 2. cast iron mould, Φ 30 mm; 3. cast iron mould, Φ 15 mm.
Slika 6. Ohlajevalne krivulje zlitine AlSi10Mg Z3 pri treh ohlajevalnih hitrostih ter njihove ustrezne mikrostrukture; 1. peščena kokila, Φ 30 mm; 2. jeklena kokila, Φ 30 mm; 3. jeklena kokila, Φ 15 mm.

rate of 0.17 °C/s was achieved. Cooling rates of approximately 5 °C/s, 40 °C/s, and 100 °C/s were achieved with the TSTA. At equilibrium cooling rate, only liquidus temperature T_L and the temperature of completed solidification T_E (the lowest temperature where the melt still exists or solidus temperature) were determined.

The differences in T_L and at T_E appeared because of different chemical compositions of alloys of researched alloys. The tendency is indicated that characteristic temperatures of solidification are dropping with the increasing cooling rate. If all three materials are compared, it can be noticed that the greatest deviation appeared at the alloy Z3. The solidification of eutectic took always place the first with the alloy Z3, followed by the alloy Z1, the last was the alloy Z2. The widest solidification range had the alloy Z2 and the narrowest the alloy Z3. The level of

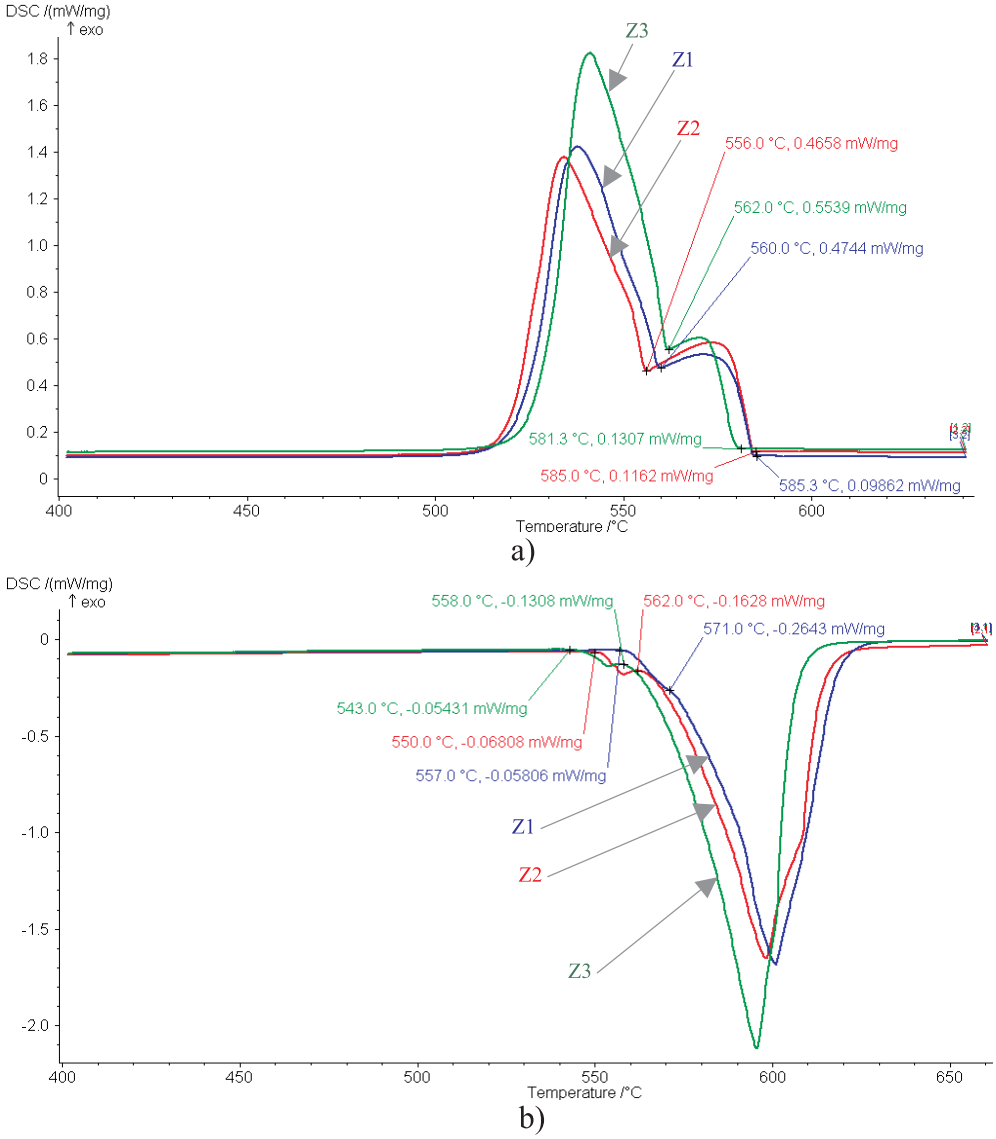

Figure 7. Cooling (a) and warming (b) curves of specimens from the simultaneous thermal analysis taken from the block.
Slika 7. Ohlajevalne (a) in ogrevne (b) krivulje simultane termične analize vzorcev vzetih iz blokov zlitin Z1, Z2 in Z3.

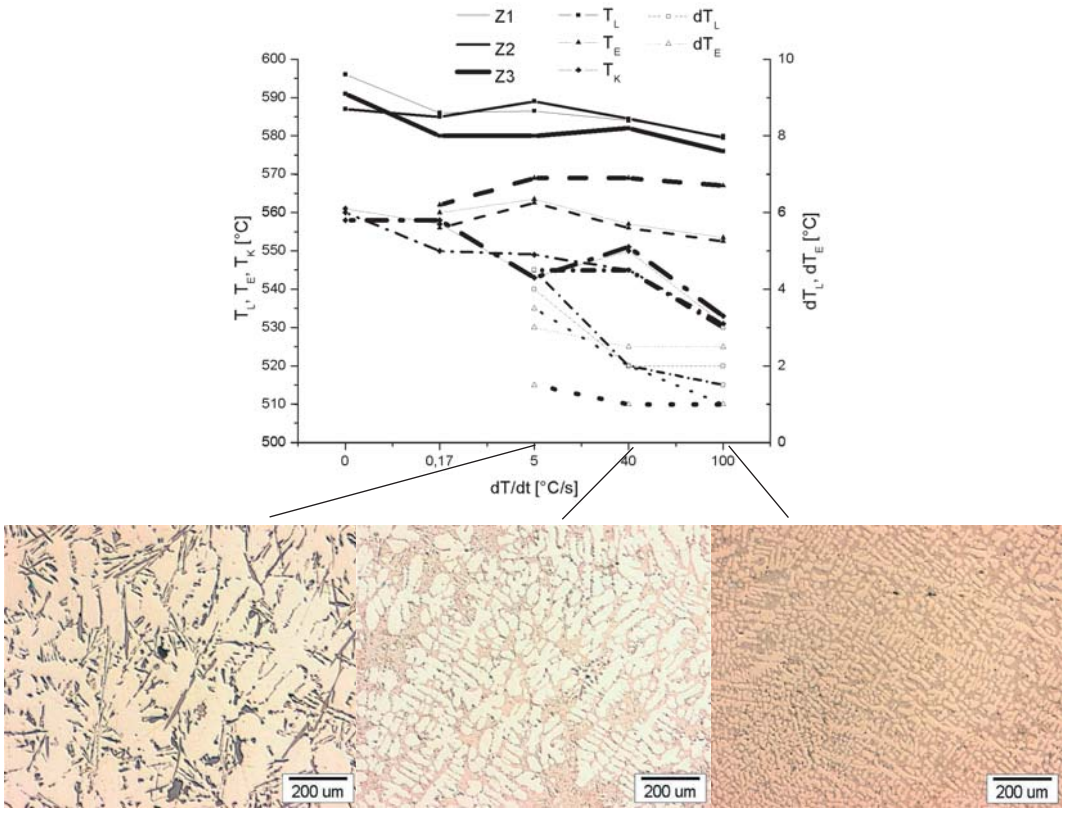

Figure 8. Graphic review of the main temperatures during solidification of alloy at triple simple thermal analyses (5 °C/s, 40 °C/s in 100 °C/s), simultaneous thermal analysis (0.17 °C/s) and at Thermo-Calc (0.01 °C/s) and their corresponding microstructures.
Slika 8. Grafični prikaz značilnih temperatur pri strjevanju zlitine iz trojne enostavne termične analize (5 °C/s, 40 °C/s in 100 °C/s), simultane termične analize (0,17 °C/s) ter Thermo-Calca (0,01 °C/s) in ustreznih mikrostruktur.

undercooling at liquidus temperatures and at eutectic temperature increased with the increasing cooling rates. The alloy Z2 had the highest liquidus and the smallest eutectic undercooling.

CONCLUSIONS

Examinations of three commercial AlSi10Mg alloys with the TSTA, STA, computer Thermo-Calc program, chemical analyses and metallographic analyses enabled several conclusions.

The variation in chemical composition of three commercial alloys has been reflected on the characteristic temperatures of the TSTA. Silicon and magnesium reduced not only liquidus temperatures, but also the temperatures of eutectic solidification (α_{Al}+ β_{Si}).

Among the metal inclusions, the most frequent in the AlSi10Mg alloy is iron that

precipitates in a shape of needles, which represents intermetallic β-Al_5FeSi phase that worsen the properties of the alloy[10]. The manganese present in the alloy prevents formation of β-Al_5FeSi phase and forms less harmful labyrinthine, α-$Al_{15}(MnFeMe)_3Si_2$ (Me=Cr,Cu), phase[10]. The alloy Z1 contained more a suitable amount of manganese with regard to iron; therefore the smallest amount of the harmful β-Al_5FeSi phase was found in alloy Z1, while the amount of α-$Al_{15}(MnFeMe)_3Si_2$ phase was the highest. In the alloys Z2 and Z3 with less manganese it had to be alloyed.

Solidification in usual practice takes place under non-equilibrium conditions, mainly because of high cooling rates. The development of microstructure depends on the chemical composition, the cooling rate and the addition of modifying elements. Highest cooling rate causes reduction of the liquidus temperatures and the temperatures of binary eutectic solidification. Small primary crystals of multicomponent solid solution based on aluminium, α_{Al} dendritic shape, and equable distribution of eutectic are formed at higher cooling rates, which improves the mechanical properties of the castings, and conditions closer to the die-casting conditions are achieved. The alloy Z2 had a larger amount of silicon, and thus the microstructure primary phase α_{Al} and binary eutectic is equally distributed, but during the solidification it formed primary silicon crystals, which is caused by the fluctuations in the melt.

The best results with the TSTA were obtained with the alloy Z3, but the microstructure was the most favorable with the alloy Z1, due to small primary crystals. Binary eutectic end α-$Al_{15}(MnFeMe)_3Si_2$ (Me=Cr,Cu) and β-Al_5FeSi phases were equally distributed among the interdendritic spaces of primary crystals α_{Al}. There was less β-Al_5FeSi phase because of the suitable amount of manganese. For use in the casting production the alloy Z1 can be recommended.

POVZETEK

Termodinamična analiza zlitine AlSi10Mg

Pri ulivanju pogosto prihaja do napak, ki povzročijo, da je ulitek neuporaben. Vzroke za livarske napake in napake v zgradbi materiala lahko iščemo v tehnologiji priprave taline na litje in v postopku litja ali pa že v samem vhodnem materialu.

Preiskovali smo zlitino AlSi10Mg proizvajalcev Z1, Z2 in Z3 in sicer s trojno enostavno termično analizo, simultano termično analizo, z računalniško simulacijo Thermo-Calc ter metalografsko analizo.

Za vsako zlitino različnih proizvajalcev smo preizkus trojne enostavne termične analize ponovili trikrat. Glede na hitrost ohlajanja smo oznakam pripisali končnico a za ohlajanje v peščeni kokili, b za ohlajanje v veliki jekleni kokili ter c za ohlajanje v mali jekleni kokili.

Kemijsko analizo smo opravljali na vhodnih materialih Z1, Z2 in Z3 ter na vzorcih po končani trojni enostavni termični analizi.

Meritve trojne enostavne termične analize so potekale v treh različnih lončkih hkrati. Uporabili smo dva merilna lončka (kokili) iz sive litine z notranjim premerom 30 mm

in z notranji premer 15 mm, tretji merilni lonček pa je bil izdelan po postopku Croning premera 30 mm. V vsak merilni lonček smo v isti višini namestili na sredino termoelement tipa K (Ni-CrNi) ter jih priključili na merilno kartico National Instruments DAQPad-MI0-16XE–50, le-to pa na osebni računalnik na katerem smo s pomočjo programskega paketa LabVIEW 5.0 zajemali merilne vrednosti ter jih sproti grafično in tabelarično beležili. Pripravljene zlitine, mase približno od 230 g do 250 g, smo stalili v grafitnem lončku s pomočjo indukcijske peči. Ko je talina dosegla temperaturo 750 °C, smo odkrili lonček, odstranili oksidno plast in vlili talino v vse tri merilne lončke.

Z računalniško aplikacijo Thermo-Calc smo izdelali simulacijo termodinamičnih ravnotežij zlitine Z1, Z2 in Z3. V programu smo izbrali ustrezno bazo podatkov, iz periodnega sistema pa izbrali elemente, ki so sestavljali našo zlitino. Program nam je izpisal vse termodinamično možne faze, ki so prisotne pri določenih pogojih in skonstruiral binarni ravnotežni fazni diagram.

Vzorci zlitin Z1, Z2 in Z3 so bili preiskani s simultano termično analizo. Na platinasti senzor aparature STA 449 firme NETZSCH smo vstavili dva enaka lončka. V en lonček smo dali preiskovani material, v drugega pa primerjalni (inertni) vzorec. Meritve smo opravljali v zaščitni atmosferi zaščitnega plina 99,999 % N_2. Vzorce smo segrevali do temperature 720 °C s hitrostjo 0,17 °C/s in jih ohlajali z enako hitrostjo do sobne temperature.

Vzorce za metalografske preiskave smo pripravili iz vzorcev od trojne enostavne termične analize. Ustrezno razrezane vzorce smo vroče vložili v umetno maso ter jih nato mehansko pripravili (brusili in polirali). Pripravljene vzorce smo nato opazovali in slikali z optičnim mikroskopom Nikon Microphot FXA, ki je opremljen s 3CCD-videokamero Hitachi HV-C20A in računalniškim programom analySIS za analizo metalografskih slik.

S termično analizo določene povprečne vrednosti hitrosti ohlajanja znašajo v peščenem lončku izdelanem po postopku Croning v območju med 4 in 6 °C/s, v jeklenem lončku premera 30 mm v območju med 30 in 45 °C/s in v jeklenem lončku premera 15 mm v območju med 90 in 110 °C/s. Ugotovili smo, da z naraščajočo ohlajevalno hitrostjo karakteriastične temperature trojne enostavne termične analize padajo, podhladitve pa se večajo.

Pri ohlajanju zasledimo s pomočjo diferenciranih ohlajevalnih krivulj izločanje faze Mg_2Si, ki se začne pri temperaturi 537 °C. Računalniška simulacija s programom Thermo-Calc nam potrdi nastajanje te faze pri temperaturi 535 °C pri Z1, pri 549 °C pri Z2 ter pri 556 °C pri Z3. Literaturni viri navajajo izločanje faze Mg_2Si pri temperaturi 554 °C.

Literaturni vir navaja možnost nastanka faze α-$Al_{15}(Fe,Mn,Me)_3Si_2$ (Me=Cr,Cu), ki jo zasledimo v mikrostrukturi kot labirintasti heterogeni zlog, z naraščajočo temperaturo litja pa je te faze manj.

Z metalografsko analizo ugotovimo, da se mikrostrukture glede na proizvajalca razlikujejo med seboj. V vzorcu iz zlitine Z2

je mikrostruktura izločenega evtektika bistveno enakomerneje razporejena v primerjavi z vzorcem iz zlitine Z1. Z naraščajočo hitrostjo ohlajanja dosežemo manjše izoblikovane primarne zmesne kristale α_{Al}, izognemo pa se nastanku iglic faze β-Al_5FeSi, ki neugodno vplivajo na mehanske lastnosti končnih ulitkov.

References

[1] Mrvar, P., Trbižan, M., Medved, J. (2001): Preiskava dimenzijskih sprememb ulitka in forme med strjevanjem modificiranih in nemodificiranih aluminijevih zlitin z dilatometrom. *Livarski vestnik*, Vol. 48, No. 5-6, pp. 131-140.

[2] Mondolfo, L. F. (1976): *Aluminum Alloys: Structure and Properties*. London, Boston, Butterworths.

[3] Tomović. M. N. (1990): *Livenje lakih i obojenih metala*. Beograd: Tehnološko-metalurški fakultet.

[4] Rosina, A. (1994): *Teorija metalurških procesov*. Ljubljana: Naravoslovnotehniška fakulteta, Oddelek za materiale in metalurgijo.

[5] *Aluminium-Taschenbuch*, 14. Auflage, Aluminium-Verlag Düsseldorf, 1993.

[6] *ASM Specialty handbook*, Aluminium and Aluminum Alloys, 1993.

[7] Villars, P., Prince, A., Okamoto, H. (1995): Handbook of Ternary Alloy Phase Diagram, ASM International.

[8] Hanemann and Schrader (1952): *Ternäre legirungen des aluminiums, Beispiele für die kristallisation ternärer systeme*, Atlas metallographicus III, 2, Verlag stahleisen M.B.H., Düsseldorf.

[9] Bäckerud, L., Chai, G., Tamminen, J. (1990): *Solidification Characteristics of Aluminum Alloys. Volume 2, Foundry Alloys*. AFS/ SKANALUMINIUM. Department of Structural Chemistry - Arrhenius Laboratory, University of Stockholm.

[10] Markoli, B., Spaić, S. and Zupanic, F. Maribor. The intermetallic phases containing transition elements in common Al-Si cast alloys, *ALUMINIUM* 80. Jahrgang 2004 ″, pp. 84-88.